ATMOSPHERIC SCIENCE LETTERS
Atmos. Sci. Let. (2008)
Published online in Wiley InterScience
(www.interscience.wiley.com) **DOI:** 10.1002/asl.186

Northern hemisphere storm tracks in strong AO anomaly winters

Ji Nie,* Peng Wang, Wenchang Yang and Benkui Tan
Laboratory of Severe Storm and Flood Disaster, Department of Atmospheric Sciences, School of Physics, Peking University, Beijing 100871, P. R., China

**Correspondence to:*
Ji Nie, Laboratory of Severe Storm and Flood Disaster, Department of Atmospheric Sciences, School of Physics, Peking University, Beijing 100871, P. R., China.
E-mail: nieji@pku.edu.cn

Received: 23 October 2007
Revised: 15 April 2008
Accepted: 21 April 2008

Abstract

Northern Hemisphere winter 300 hPa storm tracks/baroclinic waves and their energetics during strong Arctic Oscillation (AO) anomaly events are investigated. It is shown that during strong positive AO anomaly winters, the Atlantic storm track intensifies significantly and shifts northward and far downstream while Pacific storm track extends westward. Baroclinic waves over the Atlantic propagate along central North Atlantic during strong negative AO anomaly winters while during strong positive AO anomaly winters, waves over the Atlantic split into two branches. Distributions of the kinetic energy and energy conversions of different spatial scale over the storm track regions assume different characteristics for different AO phases. Copyright © 2008 Royal Meteorological Society

Keywords: **storm tracks; baroclinic wave guide; Arctic Oscillation**

1. Introduction

The storm tracks are one of the most important atmospheric systems that affect the weather and climate over the mid-latitude regions of the Northern Hemisphere and have become one of the hot research topics for the past two decades or more (e.g. the review by Chang *et al*., 2002 and the references therein). It has been now realized that there exist different timescale variability in storm track structure and intensity from seasonal (Nakamura, 1992; Christophy *et al*., 1997) to interannual (Trenberth and Hurrell, 1994; Straus and Shukla, 1997; Zhang and Held, 1999) and to interdecade (Ebisuzaki and Chelliah, 1998; Nakamura and Izumi, 1999; Geng and Sugi, 2001; Chang and Fu, 2002), which is potentially helpful to the medium- and long-term weather prediction.

As to the interannual variability, it is found that the storm track variations are closely related to ENSO cycles (Chang *et al*., 2002). In this letter, we explore by data analysis the relationship between the storm tracks and the Arctic Oscillation (AO), which is a most dominant signal in Northern Hemisphere middle and high latitudes. We focus our attention particularly on the response of the storm tracks/baroclinic wave activity at 300 hPa level to the extreme AO anomaly events in the Northern Hemisphere cool seasons from December to February. The energy and energy conversion characteristics of the storm tracks for different AO phases are examined and the contribution of the synoptic waves, planetary waves, and their interaction to the energy budget is investigated. The results obtained here throw some light on the mechanism responsible for the variation of the storm tracks of the AO phenomena.

2. Data and methods

The daily gridded 2.5° × 2.5° NCEP/NCAR reanalysis data (Kalnay *et al*., 1996) for 55 winters from DJF of 1948/1949 to 2002/2003 is used. As in Thompson and Wallace (1998), the AO index of each year is calculated on the basis of the DJF mean sea-level pressure (SLP) north of 20 °N. We choose eight maxima/minima AO index winters as strong positive/negative AO anomaly winters (SPAOAW/SNAOAW), respectively. Then, we do the composites of the storm tracks, baroclinic wave activity, the distribution of the energy and energy conversions over the eight strong positive/negative AO anomaly winters, respectively. The statistics is based on the unfiltered perturbations of the physical quantities, which are defined as the deviations from their seasonal means of each winter.

When constructing the waveguide of the baroclinic waves, we calculated the wave coherent index that is defined as the average magnitude of a pair of the strongest (either positive or negative) correlation values, one of which is observed at lag −2 upstream of the positive reference correlation center that passes the base grid at lag 0, and the other observed downstream of it at lag +2 (for more details refer Chang and Yu, 1999).

The energy budget is calculated on the basis of the eddy kinetic energy equation of the form

$$\frac{\partial K_e}{\partial t} = -\nabla\cdot(\vec{v}K_e + \vec{v}\varphi) - \alpha\omega - \vec{v}\cdot(\vec{v}_3\cdot\nabla_3)\vec{V}_m + \vec{v}\cdot\overline{(\vec{v}_3\cdot\nabla_3)\vec{v}} - \frac{\partial(\omega K_e)}{\partial p} - \frac{\partial(\omega\varphi)}{\partial p} + Res \quad (1)$$

which can be obtained following a similar way to Orlanski and Katzfey (1991). Here $\vec{V}_m$, $\vec{v}$, and ω are

the time–mean horizontal velocity, eddy horizontal velocity, and the vertical velocity in pressure coordinates, respectively. Other symbols are almost the same as in Orlanski and Katzfey (1991). The term on the left of (1) is the local tendency, the first two terms on the rhs of (1) are the divergence of kinetic energy flux and the divergence of the radiative energy flux, respectively, and the third the baroclinic conversion, the fourth and fifth are the barotropic conversion and the latter is negligible compared with the former. The sixth and seventh the vertical change of the vertical kinetic energy flux and radiative energy flux, respectively, and the last term the frictional dissipation.

In order to reveal the impact of different spatial scales on the storm track dynamics, we separate the transients into planetary waves (with zonal wavenumbers 0–3) and synoptic waves (with zonal wavenumbers greater than 3). Thus, each term in (1) can be rewritten as a sum of the synoptic wave term, planetary wave term and wave–wave interaction term. The baroclinic conversion term, e. g. can be rewritten as

$$\alpha\omega = (\alpha_s + \alpha_p)(\omega_s + \omega_p) = \alpha_s\omega_s + \alpha_p\omega_p + (\alpha_s\omega_p + \alpha_p\omega_s) \quad (2)$$

The terms on the rhs of (2) are the synoptic wave conversion, planetary wave conversion, and the conversion due to the wave–wave interaction.

3. Results

Figure 1 shows the variance of the meridional wind perturbation v' at 300 hPa level for the SPAOAW [Figure 1(a)], the SNAOAW [Figure 1(b)] and their difference [Figure 1(c)], in which the shaded region (corresponds to ≥ 250 m^2 s^{-2}) represents the mid-latitude storm tracks. Obviously the Pacific storm track extends westward during the SPAOAW *versus* the SNAOAW while the Atlantic storm track intensifies deeply and shifts northward and downstream. The significant increase occurs over the Northeast Atlantic and Europe. Similar behavior has also been observed in the relation of the Atlantic storm track and the North Atlantic oscillation (e.g. Hurrell and van Loon, 1997; Rogers, 1997).

Associated with the variation of the storm tracks is the change of the baroclinic wave activity. Figure 2 shows the schematic waveguide of the baroclinic waves at 300 hPa level. There are two bands of wave activity during the SNAOAW [Figure 2(b)], the primary one goes around the world and the secondary one runs across the Northern Asia and joins the primary waveguide at the west Pacific, which is very similar to the waveguide in the 'normal years' [Chang and Yu, 1999, figure 7(e)]. While for the SPAOAW the Atlantic part of the waveguide no longer runs along the central Atlantic as in the SNAOAW, instead it bifurcates into two branches. The northern branch goes first northeastward then eastward, joining the

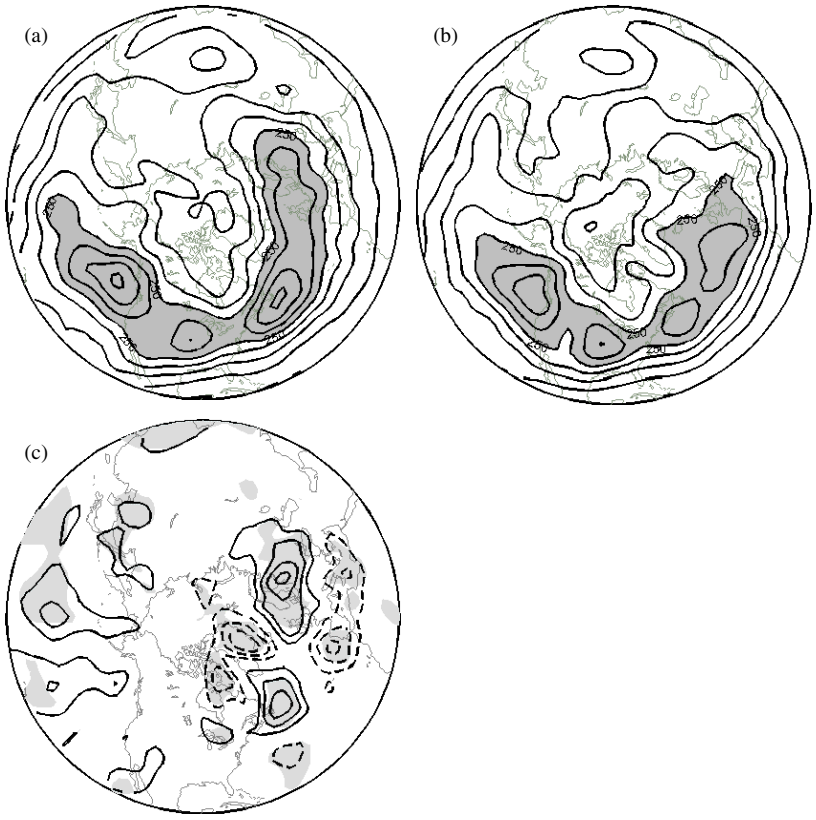

Figure 1. Variance of 300 hPa unfiltered v' averaged over eight strong positive (a) and eight negative (b) AO anomaly winters, respectively; (c) difference between (a) and (b). In (a) and (b) contour intervals are 50 m^2 s^{-2}. In (c), contour intervals are 30 m^2 s^{-2}, negative contours are shown as dashed and areas where differences are significant at the 95% level are shaded.

DOI: 10.1002/asl

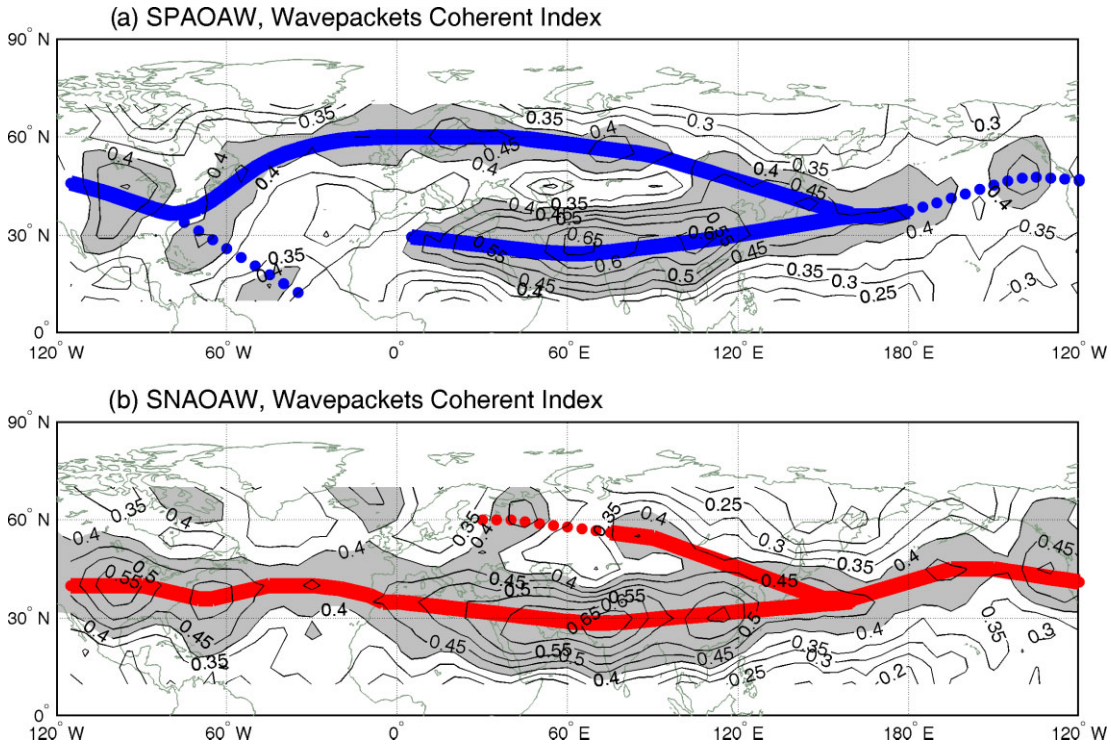

Figure 2. Wave coherence index at 300 hPa level calculated from unfiltered v' over eight strong positive (a) and eight negative AO anomaly winters (b), respectively. Contour intervals are 0.05, values over 0.4 are shaded. The red and blue bands are the schematic waveguides.

secondary waveguide over the northern Europe; while the southern branch passes southeastward into the tropics [Figure 2(a)]. It is the northern branch of the waveguide that strengthens the Atlantic storm track and causes it to shift northward and downstream.

Now we examine the energy and energy conversion characteristics of the storm tracks. Figure 3 shows the distribution of transient eddy kinetic energy at 300 hPa level for the synoptic waves [Figure 3(d) and (f)], the planetary waves [Figure 3(a) and (c)], respectively. Clearly the kinetic energy peaks of the synoptic waves are located over the storm track regions. From the SNAOAW to the SPAOAW, the Pacific peak extends westward and the Atlantic peak intensifies and shifts northward and downstream, which is in good agreement with the variation of the storm tracks. For the planetary waves during the SNAOAW their energy has two centers: the small one is located over the central Pacific and the bigger one over the Polar region and its neighboring. From SNAOAW to the SPAOAW, the central Pacific center extends northeastward and the Polar center breaks into two, which considerably enhances the planetary wave activity over the North Atlantic and Europe.

The baroclinic conversion at 300 hPa level, shown in Figure 4, is located well upstream of the storm track over the Pacific, but is just slightly upstream of the storm track over the Atlantic, as in Chang *et al*. (2002). From the SNAOAW to the SPAOAW, the conversion peak over the Atlantic intensifies and shifts northward and downstream, which is an energy source to drive the Atlantic storm track to intensify and shift. The conversion peak over the Pacific, however, contracts toward the central Pacific when the AO changes its phase from negative to positive phase [Figure 4(a) and (e)]. A close look shows that the intensification of the Atlantic conversion peak is caused mainly by an increase in the energy conversion due to the synoptic wave-planetary wave interaction term, but the contraction of the Pacific peak is due to a decrease in energy conversion due to the planetary wave term.

As to the barotropic conversion at 300 hPa level, it is generally positive over the storm track entrance regions, and negative over the exit regions [Figure 5(a) and (b)], which means that the barotropic conversion is an energy source of the storm tracks over the entrance regions and an energy sink over the exit regions, as in Chang *et al*. (2002). From the SNAOAW to the SPAOAW, the positive conversion over North America decreases deeply and the negative conversion over the Atlantic increases sharply while over the Pacific the change is only slight. From Figure 5(c) to (f) we see that the conversion by the synoptic waves is opposite in sign to the planetary waves, and the synoptic waves dominate the conversion for the magnitude of their conversion twice that of the planetary waves. The conversion due to the wave interaction is very small (the figures are omitted).

4. Conclusions

Through the composite analysis of the storm tracks and their energetics for the eight SPAOAW/SNAOAW, the following conclusions can be reached:

DOI: 10.1002/asl

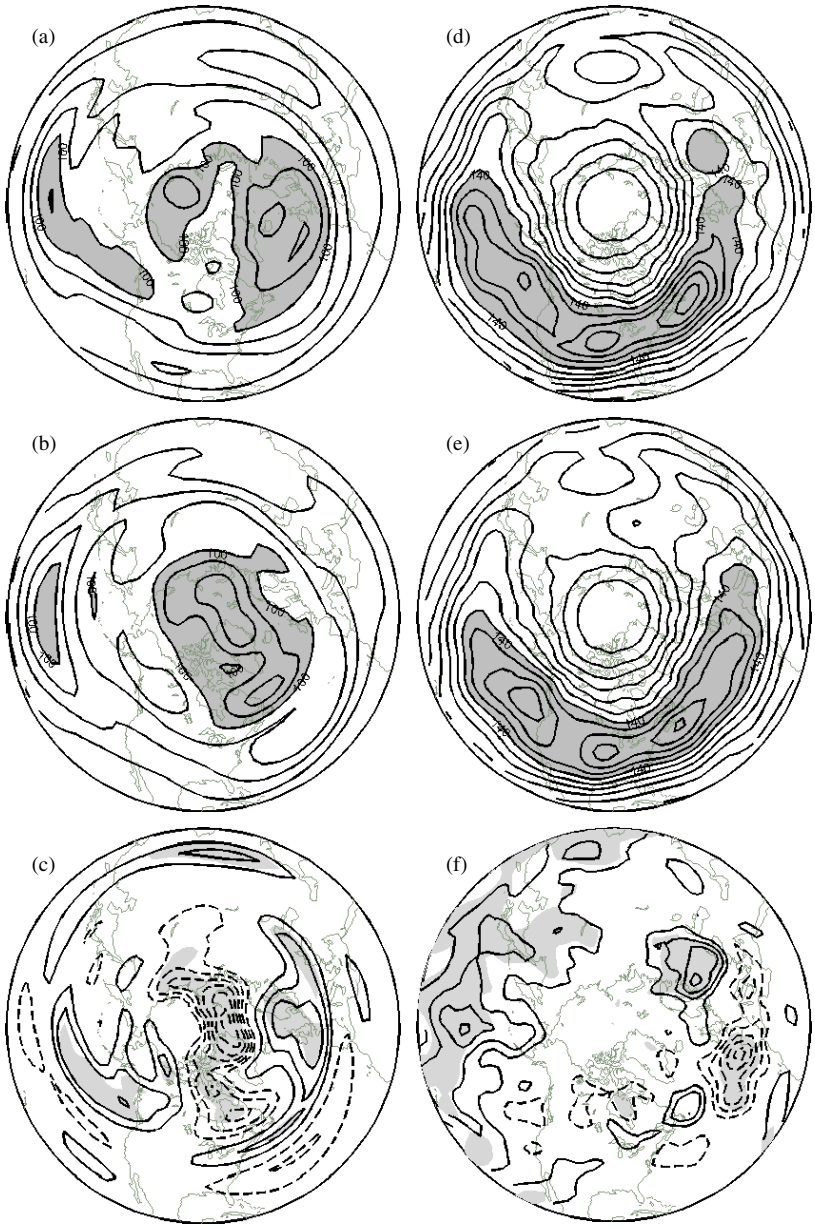

Figure 3. Kinetic energy distributions of the planetary waves at 300 hPa level for the SPAOAW (a) and the SNAOAW (b), respectively. (c) Difference of (a) and (b). (d) and (e) are kinetic energy distributions of the synoptic waves at 300 hPa level for the SPAOAW and the SNAOAW, respectively. (f) Difference of (d) and (e). In (a), (b), (d) and (e) contour intervals are 20 $m^2\ s^{-2}$. In (c) and (f), contour intervals are 10 $m^2\ s^{-2}$, negative contours are shown as dashed and areas where differences are significant at the 95% level are shaded.

1. From the SNAOAW to the SPAOAW the Pacific storm track extends westward and the Atlantic storm track intensifies and shifts northward and far downstream.
2. The baroclinic waves over the Atlantic propagate along the central Northern Atlantic track during the SNAOAW while during the SPAOAW they bifurcate into two branches.
3. The synoptic waves are more active over the central Northern Pacific, North Atlantic, and Europe during the SPAOAW than the SNAOAW while the planetary waves are more active over the northeastern Pacific, northeast Atlantic, and Europe.
4. The baroclinic conversion peak over the Atlantic intensifies and shifts northward and downstream during the SPAOAW *versus* the SNAOAW, the wave–wave interaction process is responsible for this change. From the SNAOAW to the SPAOAW the baroclinic conversion peak over the Pacific contracts toward the central Northern Pacific, and a decrease in the conversion due to the planetary wave term is responsible for the change.
5. For the barotropic conversion, the positive conversion center over America weakens considerably and the negative conversion center over the Atlantic deepens significantly during the SPAOAW than the SNAOAW, but barotropic conversion over the Pacific remains almost unchanged. The synoptic waves dominate the barotropic conversion and the wave–wave interaction term is negligible.

DOI: 10.1002/asl

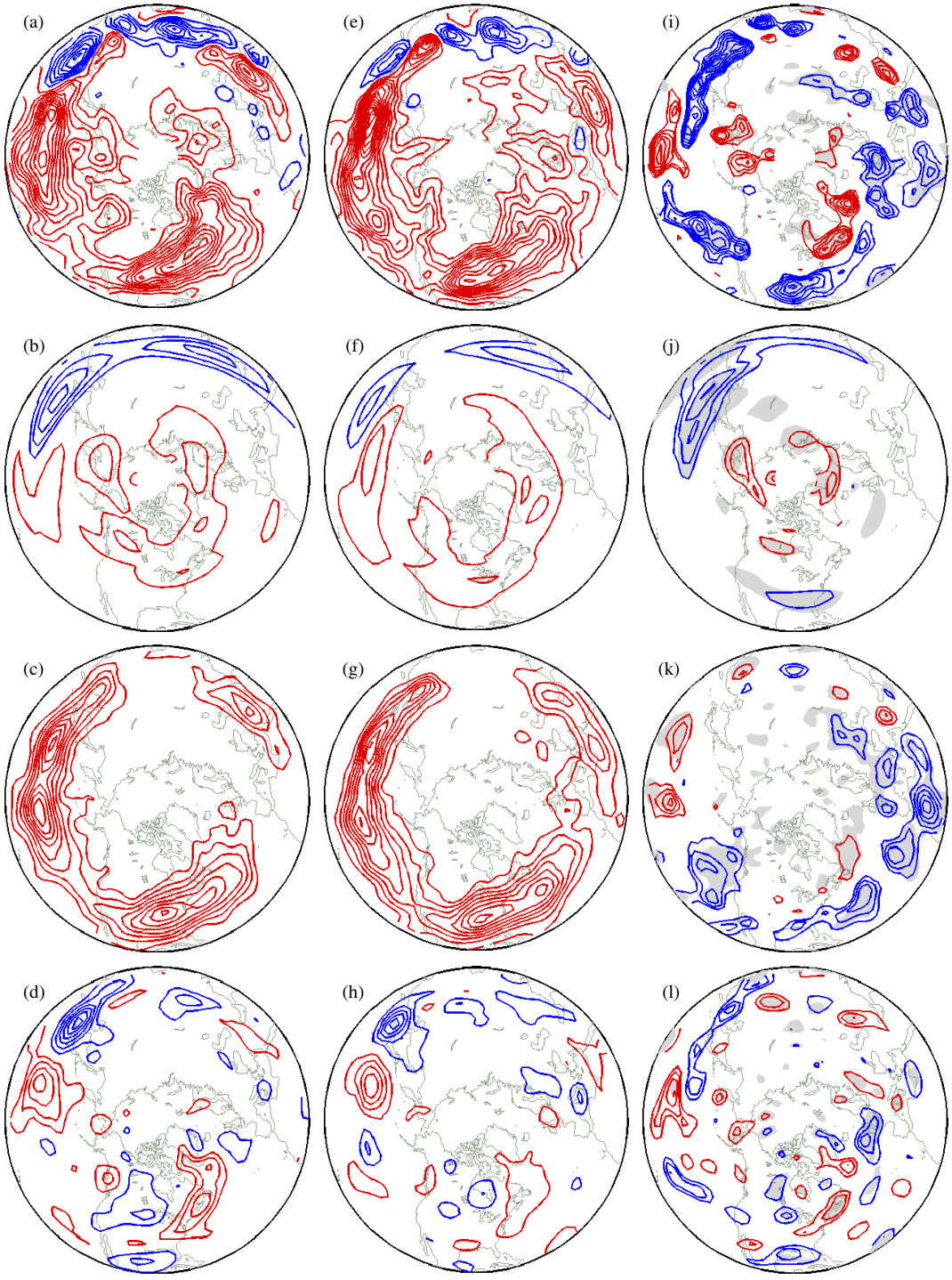

Figure 4. Distributions of the baroclinic conversion at 300 hPa level during the SPAOAW for the total wavenumbers (a), planetary waves (b), synoptic waves (c) and the baroclinic conversion due to wave–wave interactions (d), respectively. (e)~(h) are the same as in (a)~(d) except for the SNAOAW. (i)~(l) are the differences of (a)~(d) and (e)~(h), respectively. Positive contours are red and negative contours are blue. In (a)~(h) contour intervals are 10 $m^2\ s^{-2}\ day^{-1}$. In (i) ~(l) contour intervals are 5 $m^2\ s^{-2}\ day^{-1}$ and areas where differences are significant at the 90% level are shaded. In (i) contours start at 15 and in (j)~(l) contours start at 10.

It should be pointed out here that the conclusions above are based on the energy analysis at 300 hPa level. As a result they may overestimate the barotropic conversion and underestimate the baroclinic conversion for the energy budget in the troposphere as a whole for barotropic conversion peaks at upper troposphere and the baroclinic conversion reaches its maximum at low- to mid-troposphere.

It is well known that the AO and the North Atlantic oscillation (NAO) are two highly related atmospheric phenomena. Feldstein (2003), Benedict *et al*. (2004), Franzke *et al*. (2004), and Riviere and Orlanski (2007) found that the NAO is breaking and the low-frequency/high-frequency eddies' breaking plays a fundamental role in the transition of the NAO phase. Our results here show that not only

DOI: 10.1002/asl

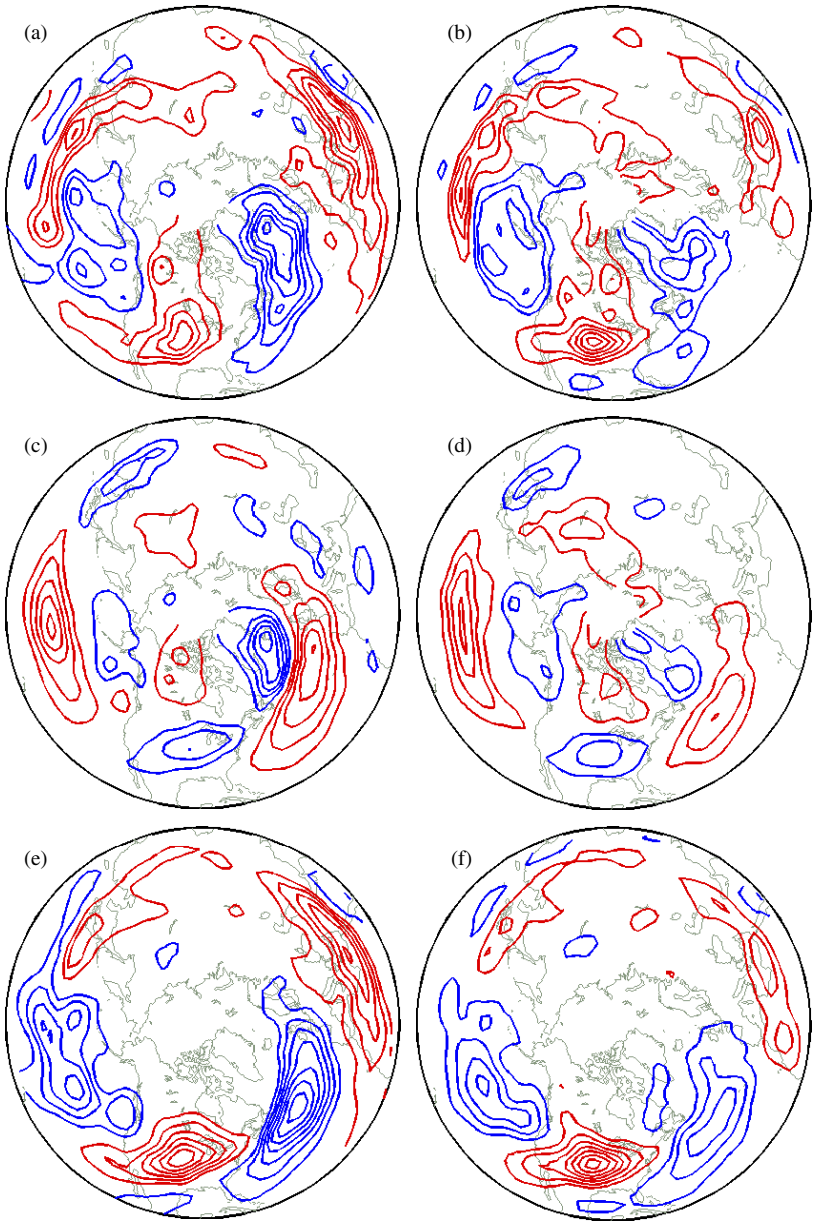

Figure 5. Distributions of the barotropic conversion at 300 hPa level during the SPAOAW for the total wavenumbers (a), the planetary waves (c), and the synoptic waves (e), respectively. (b), (d), and (f) are the same as in (a), (c), and (e) except for the SNAOAW. Contour intervals are 30 $m^2\ s^{-2}\ day^{-1}$. Positive contours are red and negative contours are blue.

the planetary waves and the synoptic waves but also their interactions play an important role in the variation in the intensity and structure of the storm tracks associated with the AO (the NAO) phenomena.

Acknowledgments

This work is supported by Project 40533016 supported by NSFC and the President's undergraduate research grant at Peking University.

References

Benedict JJ, Lee S, Felstein SB. 2004. Synoptic view of the North Atlantic Oscillation. *Journal of the Atmospheric Sciences* **61**: 121–144.

Chang EKM, Fu Y. 2002. Interdecadal variations in Northern Hemisphere winter storm track intensity. *Journal of Climate* **15**: 642–658.

Chang EKM, Lee S, Swanson KL. 2002. Storm track dynamics. *Journal of Climate* **15**: 2163–2183.

Chang EKM, Yu DB. 1999. Characteristics of wave packets in the upper troposphere. Part 1: Northern Hemisphere Winter. *Journal of the Atmospheric Sciences* **56**: 1708–1728.

Christophy M, Ulbrich U, Speth P. 1997. Midwinter suppression of Northern Hemisphere storm track activity in the real atmosphere and in GCM experiments. *Journal of the Atmospheric Sciences* **54**: 1589–1599.

Ebisuzaki W, Chelliah M. 1998. ENSO and inter-decadal variability in storm tracks over North America and vicinity. *Proceedings 23d Annual Climate Diagnostics and Prediction Workshop*. NOAA: Miami, FL; 243–246.

Feldstein SB. 2003. The dynamics of NAO teleconnection pattern growth and decay. *Quarterly Journal of the Royal Meteorological Society* **129**: 901–924.

DOI: 10.1002/asl

Franzke C, Lee S, Feldstein SB. 2004. Is the North Atlantic Oscillation a breaking wave? *Journal of the Atmospheric Sciences* **61**: 145–160.

Geng Q, Sugi M. 2001. Variability of the North Atlantic cyclone activity in winter analyzed from NECP-NCAR reanalysis data. *Journal of Climate* **14**: 3863–3873.

Hurrell JW, van Loon H. 1997. Decadal variations in climate associated with the north Atlantic oscillation. *Climatic Change* **36**: 301–326.

Kalnay ME, Kanamitsu M, Kistler R, Collins W, Deaven D, Gandin L, Iredell M, Saha S, White G, Woollen J, Zhu Y, Leetmaa A, Reynolds B, Chelliah M, Ebisuzaki W, Higgins W, Janowiak J, Mo KC, Ropelewski C, Wang J, Jenne Roy, Dennis Joseph. 1996. The NCEP/NCAR 40-year Reanalysis Project. *Bulletin of the American Meteorological Society* **77**: 437–471.

Nakamura H. 1992. Midwinter suppression of baroclinic wave activity in the Pacific. *Journal of the Atmospheric Sciences* **49**: 1629–1642.

Nakamura H, Izumi T. 1999. Out-of-phase relationship between the interannual fluctuations in poleward heat transport by the east Asian winter monsoon and Pacific stormtrack. *Preprints, 12th Conference on Atmospheric and Oceanic Fluid Dynamics*. American Meteorological Society: New York; 139–142.

Orlanski I, Katzfey J. 1991. The life cycle of a cyclone wave in the Southern Hemisphere. Part I: Eady energy budget. *Journal of the Atmospheric Sciences* **48**: 1972–1998.

Riviere G, Orlanski I. 2007. Characteristics of the Atlantic storm-track eddy activity and its relation with the North Atlantic oscillation. *Journal of the Atmospheric Sciences* **64**: 241–266.

Rogers JC. 1997. North Atlantic storm track variability and its association to the north Atlantic Oscillation and climate variability of northern Europe. *Journal of Climate* **10**: 1635–1647.

Straus DM, Shukla J. 1997. Variations of midlatitude transient dynamics associated with ENSO. *Journal of the Atmospheric Sciences* **54**: 777–790.

Thompson DWJ, Wallace JM. 1998. the Arctic Oscillation signature in the wintertime geopotential height and temperature fields. *Geophysical Research Letters* **25**: 1297–1300.

Trenberth KE, Hurrell JW. 1994. Decadal atmosphere-Ocean variations in the Pacific. *Climate Dynamics* **9**: 303–319.

Zhang YQ, Held IM. 1999. A linear stochastic model of a GCM's midlatitude storm tracks. *Journal of the Atmospheric Sciences* **56**: 3416–3435.

DOI: 10.1002/asl